Desalination and Water Treatment
www.deswater.com

doi: 10.5004/dwt.2018.23053

132 (2018) 63–74
November

Nanocomposite adsorbent based on β-cyclodextrin-PVP-clay for the removal of naproxen from aqueous solution: fixed-bed column and modeling studies

Lida Rafati[a,b], Mohammad Hassan Ehrampoush[a], Amir Abbas Rafati[c], Mehdi Mokhtari[a], Amir Hossein Mahvi[d,e,*]

[a]*Environmental Sciences and Technology Research center, Department of Environmental Health Engineering, Shahid Sadoughi University of Medical Sciences, Yazd, Iran, email: l.rafati@yahoo.com (L. Rafati), ehram2000@yahoo.com (M.H. Ehrampoush), mhimokhtari@gmail.com (M. Mokhtari)*
[b]*Deputy of Health, Hamadan University of Medical Sciences, Hamadan, Iran*
[c]*Department of Physical Chemistry, Faculty of Chemistry, Bu-Ali Sina University, P.O. Box 65174, Hamedan, Iran, email: rafati_aa@yahoo.com*
[d]*Center for Solid Waste Research (CSWR), Institute for Environmental Research (IER), Tehran University of Medical Sciences, Tehran, Iran, email: ahmahvi@yahoo.com*
[e]*Department of Environmental Health Engineering, School of Public Health, Tehran University of Medical Sciences, Tehran, Iran, Tel. +98 2144729729, Fax +98 2188950188, email: ahmahvi@yahoo.com*

Received 27 December 2017; Accepted 1 September 2018

ABSTRACT

The study of dynamics in the fixed bed column was performed using nanocomposites fabricated based on cloisite 15A, PVP and β-cyclodextrin (CD@Clay-PVP) as an adsorbent for removal of naproxen from aqueous solutions. Chemically modified nano-clay was characterized by using Fourier transform infrared spectroscopy (FTIR), scanning electron microscopy (SEM) and X-ray diffraction (XRD). The effect of different parameters of the column as well as flow rate, influent naproxen concentration and bed height were investigated to determine the adsorption characteristics by this adsorbent. Three mathematical models (bed depth service time (BDST), Thomas, Yoon–Nelson and Clark) were applied for experimental data in order to predict the breakthrough curve and determine the optimal parameters of the bed. Thomas model showed that the value of maximum solid-phase concentration decreased when the flow rate and the bed height increased but increased with increasing initial naproxen concentration. The BDST model showed that the rate constant decreased when both the bed heights and the initial concentration increased, but increased with the increase in flow rate. The value of Thomas kinetic rate constant increased with higher flow rate but decreased with increasing initial concentration and the height of the bed. The rate constant Yoon–Nelson model (K_{YN}) increased with both increasing flow rate and initial concentration but decreased with increasing bed height. Also, Clark model (R^2 = 0.9646 to 0.997) is good predicts for the breakthrough curve of naproxen adsorption process, meanwhile, the behavior of this system was simulated as a Freundlich adsorption. The value of the volumetric sorption capacity of the bed increased with increasing flow rate, initial concentration and bed height. The characteristic parameters of the relevant models for the process of designing columns were obtained using their linear and nonlinear regressions. The analysis of the error of experimental and calculated data demonstrated that all models were similar for describing the adsorption process across all adsorption conditions within the analyzed range.

Keywords: Fixed bed column; Naproxen; Adsorption; Error analysis; Breakthrough modeling

*Corresponding author.

1. Introduction

Nonsteroidal anti-inflammatory drugs (NSAIDs) such as naproxen are the most common anti-fever and anti-inflammatory drugs used in the treatment of joint, bone and muscle pains [1]. Pharmaceutical products, including NSAIDs enter into the wastewater treatment plants through Human wastes and since the treatment plants are not specially designed to eliminate drugs, these chemicals, they often remain in water and wastewater after conventional treatment [2]. Within the past two decades, several studies have reported the occurrence of new contaminants known as emerging pollutants in water and wastewater [3–5].

According to Deblond et al., among the emerging pollutants in wastewater treatment processes, the removal of NSAIDs, beta-blockers and non-steroidal anti-pain drugs are about 30–40% in different studies [6]. When NSAIDs are administered in excessive doses, they result in the formation of toxic metabolites by oxidative pathways and after oxidation they will produce toxins that are relatively unstable in aqueous media and are hydrolyzed into other toxins [7,8]. Due to the accumulative effect of contaminations and their metabolites in water systems, they are therefore eliminated from aqueous media in order to prevent their potential toxicity. Tertiary or advanced wastewater treatment systems must be used to eliminate pollutants and drugs from wastewater because conventional methods such as biological and physico-chemical treatments including coagulation, evaporation, sedimentation and filtration would be unable to remove them totally. Studies indicate that tertiary treatment including physical treatment by microfiltration (MF), nanofiltration (NF), reverse osmosis (RO), adsorption and chemical treatment using advanced oxidation processes can be effective in reducing these drugs [9–19]. Adsorption is one of the most promising techniques among the advanced treatment techniques used in eliminating and destroying NSAIDs such as naproxen from aqueous solutions [3,20,21].

Recently, surface functionalization of clays has garnered intense interest for use as solid supports due to its large surface area; fast adsorption kinetics and controllable pore size and pore arrangement in comparison to other conventional adsorbents. Although modified nano-clay has several advantages over simple clay adsorbents, it seems to be less suitable for some processes in water treatment such as column methods, due to smaller interlayer distances and inclusion complex formation abilities [22].

Chemical stability of the polymers and reproducibility of the values, also the interior cavity of the molecule provides a relatively hydrophobic environment into which a polar pollutant can be trapped are the most characteristic of β-CD [23].

The objective of this work is to synthesis and characterization of a polymer-clay composite adsorbent, functionalized with β-CD groups [24,25]. Also, a comparison of the adsorption properties of functionalized polymer-clay composite to those of clay, aiming for future applications in water and wastewater treatment. The adsorbents for naproxen were prepared using nano-clay (Cloisite 15A) as starting materials for surface modification. Firstly, there are some different methods for synthesis of polymer-clay nanocomposites and intercalation of polymer between clay layers is a common method. In the present work intercalation technique was used for fabrication of our composite adsorbent. This intercation method is based on electrostatic interaction between ionic polymer (PVP) and ionic groups on clay surface. The amount of polymer inserted between clay interlayer dependent to the some regular parameters such as polymer/clay ratio concentration, pH of solution, temperature, solvent composition, etc .

The synthesized adsorbent was used for removal of an emerging pharmaceutical pollutant (naproxen) from aqueous solution. The adsorption ability of synthesized adsorbent was studied in the removal of naproxen by fixed bed column method. Also, several mathematical models including bed depth service time (BDST), Thomas, Yoon–Nelson and Clark were applied for experimental data in order to breakthrough curve and determine the optimal parameters of the bed.

2. Material and method

2.1. Materials

Closite 15A (2M2HT) were purchased from Neutrino Co. (Iran), β-cyclodextrin from Merck (Germany), 3-aminopropyltriethoxysilane (APTS) and p–toluenesulfonyl chloride (TsCl) from Sigma-Aldrich. Naproxen pure material was prepared from Alborz bulk an Iranian pharmaceutical production company as a gift. All the other reagents were analytical grade and used without further purification. The amount of naproxen in each stage was measured using a UV-Vis spectrophotometer (PG-Instruments Ltd.) at 230 nm.

2.2. Synthesis of amino-functionalized nano-clay

In order to synthetize and prepare amino functionalized nano-clay (NH_2-Clay), 0.5 g of Closite 15A and 2.5 moles of APTS and 25 ml of toluene were refluxed for at least 2 h. The resulting slurry was filtered and washed with acetone in order to remove the unreacted materials and was dried in the oven at 150ºC for 2 h. Next, the resulting precipitate was dissolved in 70 ml of distilled water and was stirred for 30 min for removed any residual organosilane. Finally, the obtained NH_2-Clay was isolated by centrifugation of 2000 rpm and was dried in the oven at 150ºC.

2.3. Preparation of 6-mono-(p-toluenesulfonyl)-β-cyclodextrin (Ts-βCD)

Monotosyl-β-cyclodextrin (Ts-βCD) was synthesized and prepared as follows: 18 g of β-CD (16 mmol) was dissolved in 100 ml of dry pyridine and then 2.5 g of p-toluenesulfonyl chloride (12 mmol) was added to the solution. The reaction was refluxed for 8 h at 2 – 4ºC and then it was kept at room temperature for 2 d. After concentrating the solution under vacuum condition, the mixture was poured in diethyl ether. The resulting white precipitate was collected and repeatedly rinsed with distilled water. Finally, the obtained material was washed by acetone and was dried in the oven under vacuum condition at 60ºC.

2.4. Preparation of clay-grafted β-CD (CD@Clay)

50 ml of dimethyl formamide (DMF) containing 2 g of NH_2–Clay was kept in a three neck flask equipped with reflux condenser at room temperature. Then, 0.25 g of Ts-βCD was added to 10 ml DMF and was added to the initial mixture at pH = 7–8. The temperature was increased to 60°C. The reaction was stirred with a magnetic stirrer for 7 h under nitrogen atmosphere. Subsequently, the product was filtered, washed with DMF and acetone to remove any unreactive and dried in a drying cabinet for 24 h at 60°C to eliminate the solvent.

2.5. Preparation of the intercalate CD@Clay-PVP

A suspension of 0.5 g CD@Clay in 15 ml of toluene was added dropwise to a solution of 0.05 g polyvinylpyrrolidone (PVP) in 15 ml toluene with ultrasonication for 1 h. The resulting mixture was kept at room temperature for one day. The mixture was centrifuged, washed three times with toluene and dried in the oven at 60°C overnight (scheme 1).

2.6. Characterization

The FT-IR spectra were recorded by a Perkin–Elmer FT-IR spectrophotometer (model Spectrum GX). The spectrum was recorded from 550 to 4000 cm^{-1} using KBr pellets. The crystallinity of the nanoclay materials was characterized by X-ray diffraction (XRD; ITAL structures model APD2000) with applying Cu Kα radiation wavelength 0.15405 nm. A step size of 0.01 and a time per step of 0.2 s were used. Diffraction patterns were taken over the 2 h range 0–60°. The sizes and morphologies of the synthesized nanoadsorbents were examined by scanning electron microscopy (SEM) image that obtained with a MIRA3 TESCAN HV: 20.0 KV from Czech Republic.

2.7. Fixed bed column adsorption experiments

Fixed-bed column of glass, with an inner diameter of 1 cm and a height of 30 cm was filled and prepared by a certain amount of adsorbent for column experiments. In order not to prevent the outflow of adsorbent from the column during the flow of fluid, the end of the column was covered by polyethylene wool. At first, synthesized nanoadsorbent was used in the column and it was observed that high adhesion of nanoadsorbent caused blockage in fixed-bed column so the adsorbent with Ottawa sand (OS) (ASTM 20–30; 95% OS and 5% CD@Clay-PVP adsorbent) was placed in the column. Table 1 shows some characteristics and properties of the OS. In order to determine the rate of adsorption of

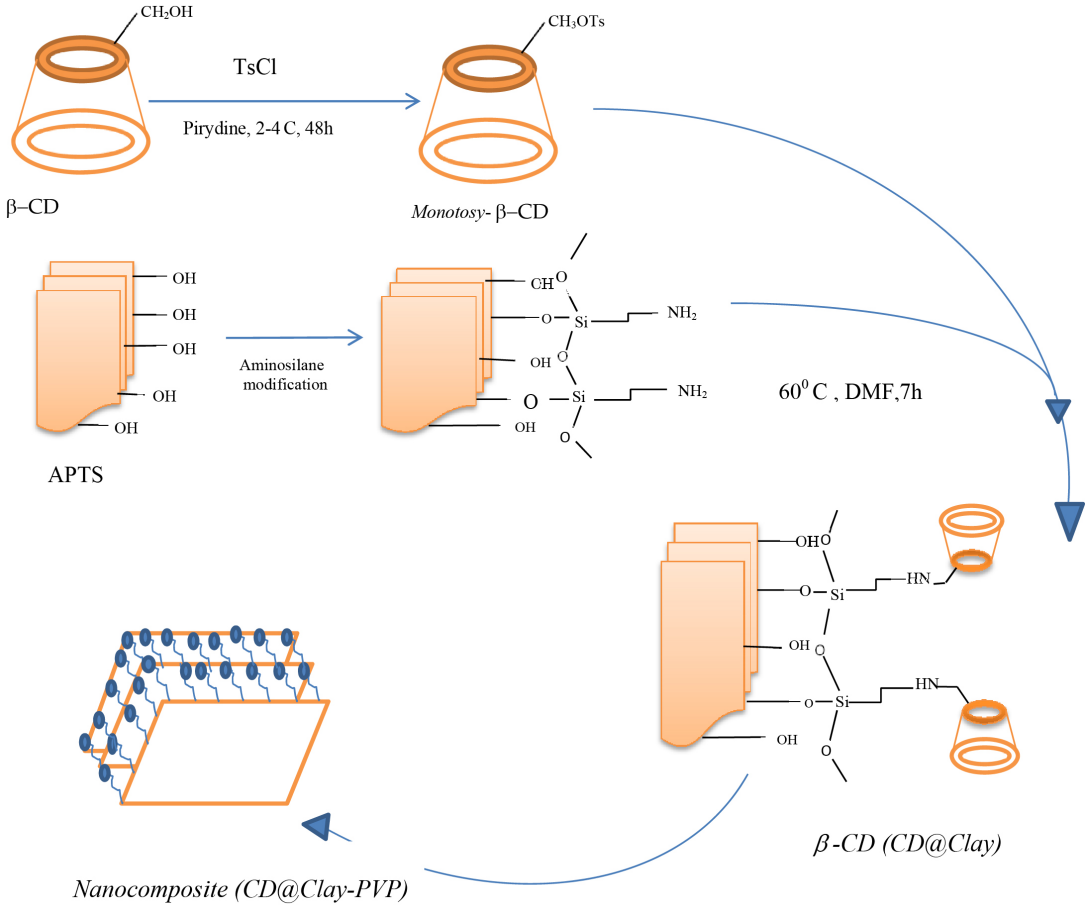

Scheme 1. Schematic procedure for synthesis of CD@Clay-PVP.

Table 1
Physical characteristics of Ottawa sand (OS)

Characteristic	Ottawa sand
Specific gravity	2.64
D10 (mm)	0.29
Dc (mm)	0.38
D50 (mm)	0.43
D60 (mm)	0.46
Coefficient of uniformity	1.58
Coefficient of curvature	1.08
USCS symbol	SP
C_{max}	0.69
C_{min}	0.51

naproxen by OS, first separate column was launched by OS. Before the experiment started, the column was filled by a known weight of a mixture containing adsorbent and OS, dispersed in deionized water in downward flow direction to withdraw the trapped air between the adsorbent particles. Then, naproxen working solutions were continuously fed downward into the column and the samples were collected from the bottom of the column at different time stored at 4°C until analysis by UV-Vis spectrophotometer.

2.8. Effect of bed height

To evaluate the effect of the bed height, it is necessary to analyze the breakthrough curve (BTC). The time for break through appearance and shape of BTC are very important characteristics for determining the operation and the dynamic response of an adsorption column [26,27]. The shape of the concentration-time profile of BTC is the important characteristic for adsorption dynamic response and process design of an adsorption column [26].

It can be done by calculating breakthrough curve parameters. The breakthrough curves for adsorption of naproxen at different amounts of adsorbent in column (1, 1.5 and 2 g corresponding to 1.5, 2 and 2.5 cm bed height, respectively) with a constant flow rate of 6 mL/min, the empty bed contact time (EBCT) = 1.96 min and the initial concentration of naproxen 3 mg/LL were evaluated. The effluent was collected for naproxen analysis.

2.9. Effect of flow rate on breakthrough curve performance

The effect of flow rate on the naproxen removal in fixed-bed column with a bed depth of 1.5 cm, the initial concentration of 3 mg/LL and EBCT = (1.96 and 1.3 min) was investigated. The experiment was carried out at two different flow rates (6 and 9 mL/min).

2.10. Effect of initial naproxen concentration

The effect of initial naproxen concentration on the breakthrough curves was investigated using feed solutions of initial naproxen concentrations of 3, 5 and 10 mg/LL. The investigation was performed using fixed beds with a bed depth of 1.5 cm, Q = 6 mL/min and EBCT = 1.96 min.

2.11. Mathematical description of fixed bed column studies

The behavior of column for adsorption of an adsorbate is described in terms of an "effluent concentration-time" profile, which is called the breakthrough curve. The time of breakthrough is defined as the time when the outlet adsorbate concentration equals a certain fraction of the original adsorbate concentration at the inlet of the column. The breakthrough curves were expressed in terms of normalized concentration, defined as the ratio of the outlet concentration, C_t, to the feed concentration, C_0, as a function of time.

The total adsorbed drug (q_{total}) by the column can be obtained by integrating the plot of adsorbed concentration (C_{ad}) vs. the flow time [22]:

$$q_{total}\left(mg\right)=\frac{QA}{1000}=\frac{Q}{1000}\int_{t=0}^{t=t_{total}}C_{ad}dt \tag{1}$$

where t_{total}, Q, and C_{ad} are the total time for the column to reach saturation (min), volumetric flow rate (ml/min), and the difference in the naproxen concentration at the initial time and the t time caused by adsorption (mg/LL), respectively. The total amount of adsorbate delivered to the column system (m_{total}) is obtained from the following equation [11,30]:

$$m_{total}\left(mg\right)=\frac{C_0Qt_{total}}{1000} \tag{2}$$

From the column data, one can determine the equilibrium adsorption. Also, this quantity was used to obtain the capacity of adsorbent required to remove drug. The equilibrium drug uptake (q_e), also known as the column maximum capacity, was calculated by the following equation:

$$q_e=\frac{q_{tot}}{M} \tag{3}$$

where M is the amount of adsorbent (*CD@Clay-PVP*) packed in the column (g). The removal percentage of naproxen can be obtained from Eq. (4) (33):

$$R\left(\%\right)=\frac{q_{tot}}{m_{total}}\times 100 \tag{4}$$

2.12. Dynamic adsorption models

Modeling of data available from column studies facilitates scale-up potential. Successful design of a column sorption process requires the accurate prediction of the concentration–time profile or breakthrough curve of the effluent. Several simple mathematical models have been

developed to describe and possibly predict the dynamic behavior of the bed in column performance [30].

In order to describe the fixed-bed column behavior, four classic kinetic models, bed depth service time (BDST), Thomas, Yoon–Nelson and Clark models were used to fit the experimental data in the column.

2.12.1. Bed depth service time (BDST) model

Bed depth service time (BDST) is a simple model that states that column bed depth and service time bears a linear relationship in terms of process concentration and adsorption parameters. This model was proposed by Hutchins [31] after modification of Bohart-Adams model [32]. In fact, this model is simplified the Bohart–Adams equation and presented a linear relationship between the bed depth and service time. The linear expression of BDST model can be expressed as follows [30]:

$$t = \left(\frac{N_0 H_T}{C_0 U}\right) - \left(\frac{1}{k_0 C_0}\right)\ln\left(\frac{C_0}{C_t} - 1\right) \tag{5}$$

where C_t is the effluent concentration of solute in the liquid phase (mg L^{-1}), C_0 is the inlet solute concentration (mg L^{-1}), U is the influent linear velocity (cm min^{-1}), N_0 is the adsorption capacity (mg L^{-1}), k_0 is the rate constant in BDST model (L mg^{-1} min^{-1}), t is time (min), and H_T is the bed height of column (cm). From the plots of time vs. bed height (H_T), the BDST parameters, namely N_0 and k_o, can be determined.

2.12.2. Thomas model

Thomas model [33] is widely used to evaluate the performance of adsorption fixed-bed columns and the influencing adsorption parameters of the column system. This model is obtained from the equation of conservation of mass in a flow system. The model assumption is that the second-order reaction kinetics is reversible and follows the Langmuir kinetics of adsorption. On the other hand, the suitability of the Thomas model may be explained in that this model assumes negligible axial dispersion in the column adsorption since the rate driving force obeys second-order reversible reaction kinetics [34]. In addition, the Thomas model considers that sorption is not limited by the chemical reaction, but is controlled by the surface reaction between the adsorbed and empty capacity of adsorbent. The Thomas model is expressed in a linearized form, as follows [35]:

$$\ln\left(\frac{C_0}{C_t} - 1\right) = \left(\frac{k_{Th} q_0 M}{Q}\right) - \left(\frac{k_{Th} C_0 V_{eff}}{Q}\right) \tag{6}$$

where k_{Th} is the Thomas rate constant (ml min^{-1} mg^{-1}), C_0 is the inlet naproxen concentration (mg/LL), C_t is the effluent naproxen concentration (mg/LL), q_0 is the maximum solid phase concentration (mg/g), V_{eff} is the throughput volume (ml), M is the amount of adsorbent in the column (g) and Q is the flow rate (ml/min). The value of k_{Th} and q_0 can be obtained from the plot of $\ln(C_0/C_t - 1)$ versus V_{eff} (ml).

2.12.3. Yoon–Nelson model

The Yoon–Nelson model was developed based on the assumption that the rate of decrease of the probability of adsorption for each adsorbate molecule is proportional to the probability of adsorption and of adsorbate breakthrough on the adsorbent. This model is known to be a simple theoretical model because less column data is needed for the construction of the model and does not require detailed data regarding to the characteristics of the sorbate, the type of the sorbent and physical properties of the sorption bed [36, 37]. This model is suitable for the single component system [38]. The linearized Yoon–Nelson equation is given below:

$$\ln\frac{C_t}{C_0 - C_t} = k_{YN} t - \tau k_{YN} \tag{7}$$

where k_{YN} is the rate constant (min^{-1}) and τ is the time required for 50% exchange breakthrough (min). The values of k_{YN} and τ can be determined by plotting $\ln [C_t/(C_0 - C_t)]$ vs. t.

2.12.4. Clark model

The Clark model has been proposed for modeling the breakthrough curves in fixed bed adsorption based on a combination of bed differential mass balances to estimate a mass transfer flux and the assumption of Freundlich-type equilibrium at the column inlet [39]. It assumes plug flow and negligible dispersion phenomena [40]. The foundational equations are given as follows:

$$\frac{C}{C_0} = \left(\frac{1}{1 + Ae^{-rt}}\right)^{\frac{1}{n}-1} \tag{8}$$

With

$$A = \left(\frac{C_0^{n-1}}{C_b^{n-1}}\right) e^{rt_b} \tag{9}$$

and

$$r = \frac{\beta}{\cup} v_m (n-1) \tag{10}$$

where n is the Freundlich constant, and C_b is the solute concentration (mol m^{-3}) at breakthrough time, t_b (h), and u_m is the migration velocity of the concentration front in the bed (cm/h). The A_C and r_C are known as the Clark constants. The linearized form of the Clark model is as follows:

$$\ln\left[\left(\frac{C_0}{C}\right)^{n-1} - 1\right] = -rt + \ln A \tag{11}$$

From a plot of $\ln\left[\left(\frac{C_0}{C}\right)^{n-1} - 1\right]$ against t at a given bed height and flow rate, the values of A and r can be obtained [39].

2.13. Error Analysis

In order to verify the model for the adsorption system, it is necessary to analyze the data using error analysis. A number of error functions employed in this study are included: the coefficient of determination (R^2), the sum of the square of the error (*SSE*), residual root mean square error (*RMSE*), the sum of the absolute error (*SAE*), average relative error (*ARE*) and the average relative standard error (*ARS*). The smaller the error function value, the better the curve fitting. The calculated expressions of some error functions are as follows [41–44]:

Residual root mean square error (RMSE):

$$\mathrm{RMSE} = \sqrt{\frac{1}{n-2}\sum_{i=1}^{n}\left(Y_{exp} - Y_{cal}\right)^2} \tag{12}$$

where n is the number of experimental data points, Y_{cal} is the predicted (calculated) data and Y_{exp} is the experimental data and Y represents the ratio C_t/C_0.

(ii) The coefficient of determination (R^2):

$$R^2 = \frac{\left(Y_{exp} - \overline{Y_{cal}}\right)^2}{\sum_{i=1}^{n}\left(Y_{exp} - \overline{Y_{cal}}\right)^2 + \left(Y_{exp} - Y_{cal}\right)^2} \tag{13}$$

where $\overline{Y_{cal}}$ is the average of Y_{cal}.

(iii) The sum of the square of the error (*SSE*):

$$SSE = \sum_{i=1}^{n}\left(Y_{exp} - Y_{cal}\right)^2 \tag{14}$$

(iv) The sum of the absolute error (*SAE*):

$$SAE = \sum_{i=1}^{n}\left|Y_{cal} - Y_{exp}\right|_i \tag{15}$$

(v) Average relative error (*ARE*):

$$ARE = \frac{1}{n}\sum_{i=1}^{n}\left|\frac{Y_{cal} - Y_{exp}}{Y_{exp}}\right| \tag{16}$$

(vi) The average relative standard error (*ARS*):

$$\mathrm{ARS} = \sqrt{\frac{\sum_{i=1}^{n}\left(Y_{cal} - Y_{exp}/Y_{exp}\right)^2}{n-1}} \tag{17}$$

3. Results and discussion

3.1. Characterization of CD@Clay-PVP adsorbent

Scheme 1 shows the overall procedure used to synthesize clay nanocomposite functionalized with β-CD. The FT-IR spectra of the clay (a), amino functionalized clay (b), CD-Clay (c), PVP (d) and CD@Clay-PVP (e) are shown in Fig. 1. Nanocomposite (CD@Clay-PVP) IR spectrum showed bands which could be recognized on b-CD, PVP and Cloisite 15A spectra. For example, the band at 1058 cm^{-1} on cloisite 15A (Si–O stretching vibration) was absent on β-CD and PVP spectrum but present on nanocomposite. The silylated Cloisite 15A clay has characteristic peaks at 1058, 529, and 467 cm^{-1} originating from the Si–O group. The bands at 1696 cm^{-1} (C = O stretching vibration) on PVP was absent on clay and β-CD but present on nanocomposite. Also, the clay has IR peak at 3645 cm^{-1} corresponding to the free O–H group. The peaks at 2932 and 2861 cm^{-1} are due to the alkyl chains of the organic modifier in the clay. Meanwhile, the nanocomposite has the following IR peaks: characteristic CH_2 (2932, 2861 cm^{-1}) and Si–O (1058, 529, and 467 cm^{-1}) peaks that are intrinsic to the polymer and the clay, respectively.

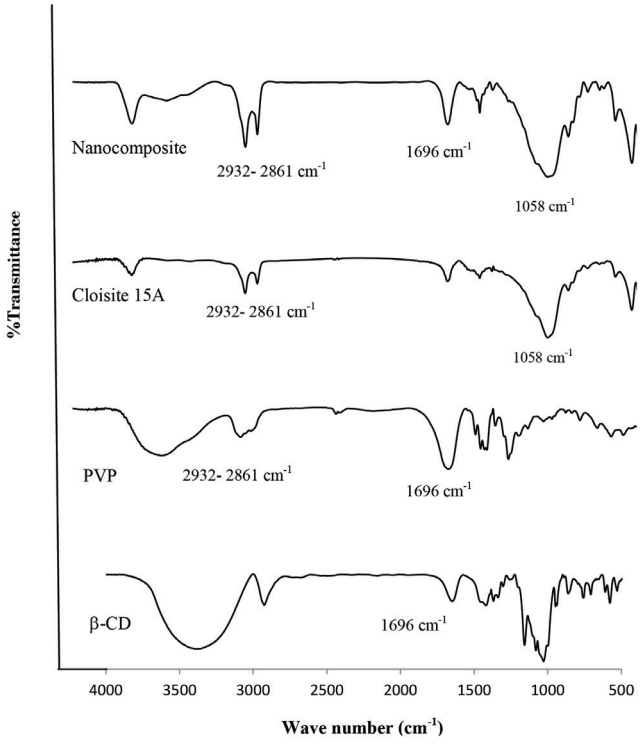

Fig. 1. The FT-IR spectra of the cyclodextrin, PVP, cloisite 15A, CD-Clay and CD@Clay-PVP.

The SEM technique was used to investigate the surface morphologies of the prepared samples. The surface morphologies of the clay nanopowder and the fabricated functionalized clay nanocomposite with the PVP (CD@Clay-PVP) are shown in Fig. 2. The SEM images of the fabricated clay nanocomposite (CD@Clay-PVP) in Fig. 2b show different surface morphologies than that of the clay nanopowder (Fig. 2a). It is noticed that the inter layer spaces are more increased in Fig. 2b which indicate the impregnation of the nanostructure of the polymeric between the clay layers.

XRD patterns of the clay nanopowder and the clay nanocomposite with PVP are represented in Fig. 3. The characteristic features of these patterns are (a) the clay nanopowder has a peak at 2θ = 7.3° which is corresponding to (001) crystallographic plane of its crystal structure and the layer distance of clay is 1.21 nm; (b) peak at 2θ = 2.9° which is corresponding to the MMT layer distance of 3.04 nm. Compared with cloisite 15A, CD@Clay-PVP show

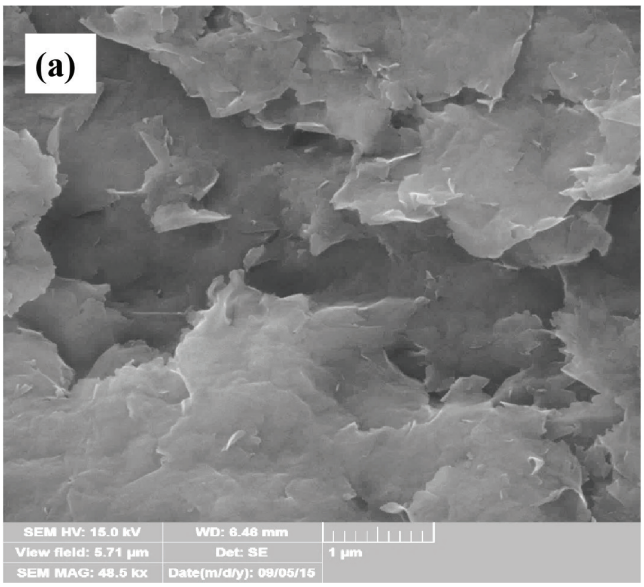

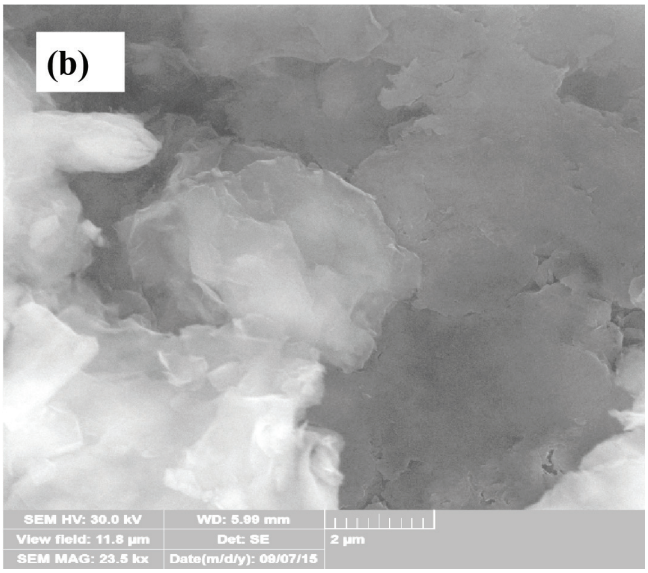

Fig. 2. SEM images of (2a) Closite 15A and (2b) CD@Clay-PVP nanocomposite.

higher interlayer distances that indicates polymer has intercalated into MMT's layers successfully.

The CD@Clay-PVP composite showed a peak shift towards a lower diffraction angle (2θ) than the pure cloisite 15A, indicating an increase in the interlayer spacing of silicate layers and intercalation of polymer chains between clay layers. The reduced peak intensity is attributed to the low concentration of clay in the samples. The shift in the peak from a higher to a lower diffraction angle has been reported by different researchers [45,46].

3.2. Column studies

Performance of continuous fixed-bed column system is expressed through breakthrough curve. The behavior of the desired column for adsorption of naproxen was expressed

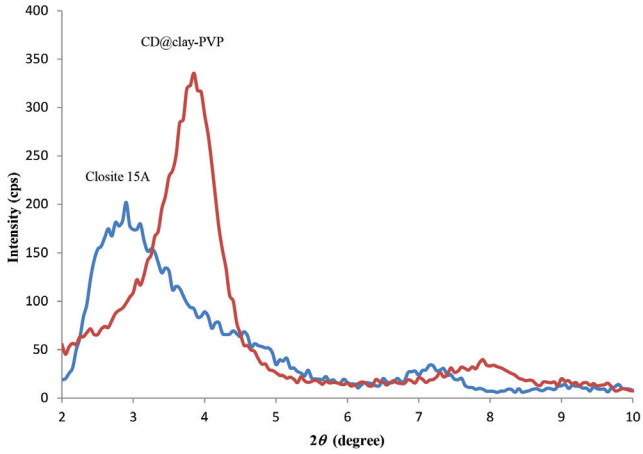

Fig. 3. XRD patterns of Closite 15A and CD@Clay-PVP nanocomposite.

as the plot of C_t/C_0 as a function of time, t, or column output volume in the desired conditions. Then, the obtained data were evaluated by mathematical models associated with the fixed-bed column system. The removal percentage of naproxen and related parameters are shown in Table 2.

As noted, at first the separate columns of OS were launched and it was proved that OS had no effect on concentration reduction or elimination of naproxen. Therefore, these materials were only used to prevent the column by nano-composite adsorbent and played the role of facilitator. Performance of new nano-composite adsorbent (CD@Clay-PVP) was compared with some other adsorbents previously reported for removal of naproxen in Table 3.

3.3. Effect of bed height on BTC

The accumulation of adsorbate in a fixed-bed column is dependent on the quantity of adsorbent inside the column, and the steepness of all the BTCs is a strong function of bed height. In order to find out the effect of bed height on the BTC, sample solution having influent naproxen concentration 3 mg L^{-1} and flow rate 6 mL min^{-1} was passed through the column by varying the bed height. Fig. 4a represents the performance of breakthrough curves at various bed heights i.e. 1.5, 2 and 2.5 cm. As can be seen from Fig. 4a, the breakthrough time was increased with increasing the bed height. BTCs parameters for naproxen column study were tabulated in Table 2. As shown in Table 2, the bed depth strongly influenced the naproxen uptake capacity of 3.49, 3.4 and 3.38 mg/g, which was recorded at 1.5, 2 and 2.5 cm, respectively. Also, the results revealed that the breakthrough time increased from 450 min to 383 min, with increasing bed height from 1.5 to 2.5 cm. Higher uptake was observed at the highest bed height due to an increase in the surface area of adsorbent (CD@Clay-PVP), which provided increased availability of binding sites for the attachment of naproxen molecules for adsorption process [47]. Also, the bed capacity and adsorption efficiency increased with increasing bed height. On the other hand, as the bed depth increased, effluent volume (V_{eff}) increased, which might be due to

Table 2
Parameters in fixed-bed column for naproxen adsorption by CD@Clay-PVP

C_0 (mg/LL)	Q (ml/min)	H_T (cm)	t_{total} (min)	m_{total} (mg)	q_{total} (mg)	q_e (mg/g)	V_{eff} (ml)	*EBCT* (min)	*MTZ** or H_{UNB} (cm)	H_B** (cm)
3	6	1.5	383.33	6.9	3.49	3.49	2300	1.96	1.305	0.195
3	6	2.0	416.66	7.5	5.10	3.40	2500	1.96	1.436	0.564
3	6	2.5	450.00	8.1	6.76	3.38	2700	1.96	1.685	0.817
3	6	1.5	383.33	6.9	3.49	3.49	2300	1.96	1.305	0.195
5	6	1.5	316.66	9.5	5.67	5.67	1900	1.96	1.275	0.225
10	6	1.5	291.66	17.5	11.43	11.43	1750	1.96	0.969	0.532
3	6	1.5	383.33	6.9	3.49	3.49	2300	1.96	1.305	0.195
3	9	1.5	177.77	4.8	2.28	2.28	1600	1.30	0.651	0.849

*The unused bed length (HUNB) or Mass Transfer Zone (MTZ).
**The used bed length HB (up to the break point).

Table 3
Comparison of our developed nano-composite adsorbent performance with some recently reported adsorbents

Adsorbate	Adsorbent	%Removal	Reference
Naproxen	Activated biochar	97.7%	[44]
	Commercially powdered activated carbon (PAC)	94.1%	[44]
	Amberlite XAD–7	60%	[45]
	Granular Activated Carbon (GAC)	90%	[46]
	Molecularly imprinted polymer (MIP)	38%	[47]
	Octolig®	90%	[48]
	Octolig and selected metalloligs	90%	[49]
	Porous sugarcane bagasse (PSB)	83.11%	[50]
	CD@Clay-PVP	99.8%	This work

the more contact time [48]. Fig. 4a shows that the slope of breakthrough curve decreased with increasing bed depth, which resulted in a broadened mass transfer zone [49–51].

3.4. Effect of flow rate

It is well known that the flow rate is an important parameter as it controls the contact time between the solute and adsorbent surface. Furthermore, the residence time of the solute in the fixed bed is directly proportional to the flow rate, and a large residence time will allow greater amounts of adsorbate to be adsorbed. The effect of flow rates on the breakthrough curves was investigated using flow rates of 6 and 9 mL/min. The breakthrough curves at various flow rates of naproxen are shown in Fig. 4b. As indicated in Fig. 4b, the breakthrough curve became faster as the flow rate increased. In all cases, a feed solution having an initial naproxen concentration of 3 mg/LL was passed through a fixed bed of depth 1.5 cm. It can be seen that as the flow rate was increased from 6 to 9 mL/min, the EBCT decreased from 1.96 to 1.3 min and the exhaust time (corresponding to 98% of influent concentration) was found to be decreased from 383 to 177 min.

The faster breakthrough curve was due to this fact that at a high rate of influent naproxen did not have enough time to contact with adsorbent, which resulted in a lower removal of naproxen in column. Thus, the contact time of naproxen with CD@Clay-PVP is very short at higher flow rate resulting in a lower degree of adsorption leading to an increase in the effluent drug concentration [47].

On the other hand, the influent flow rate also strongly influenced the drug uptake capacity. Obtained results for adsorption of naproxen on CD@Clay-PVP showed that flow rates had some negative effects on the adsorption capacity. The amount of total naproxen uptake (q_e) decreased from 3.49 to 2.28 mg/g as flow rate increased from 6 to 9 mL/min.

3.5. Effect of initial concentration

The performance of adsorption column for different input concentrations of naproxen (3, 5 and 10 mg/LL) was examined at the flow rate of 6 mL/min and adsorbent amount of 1 g (adsorbent height in column 1.5 cm). The results showed that as the initial concentration of naproxen increases, the breakthrough time decreases (Fig. 4c) because the high concentration of naproxen saturates adsorption column faster and adsorbent particles are exposed to further milligrams of the adsorbate. As the concentration of naproxen increases, sharper breakthrough curves are obtained which indicates smaller area of mass transfer and higher adsorption rate. Lower concentration than the input naproxen causes delay in the curve because at lower concentration the concentration difference for the transfer of naproxen decreases. The driving force for adsorption is the concentration difference of adsorbate on adsorbent and adsorbate in the solution. Higher concentration difference creates greater chemical potential that is optimal for adsorption process. Moreover, concentration changes will affect column saturation rate and breakthrough time, as well [27].

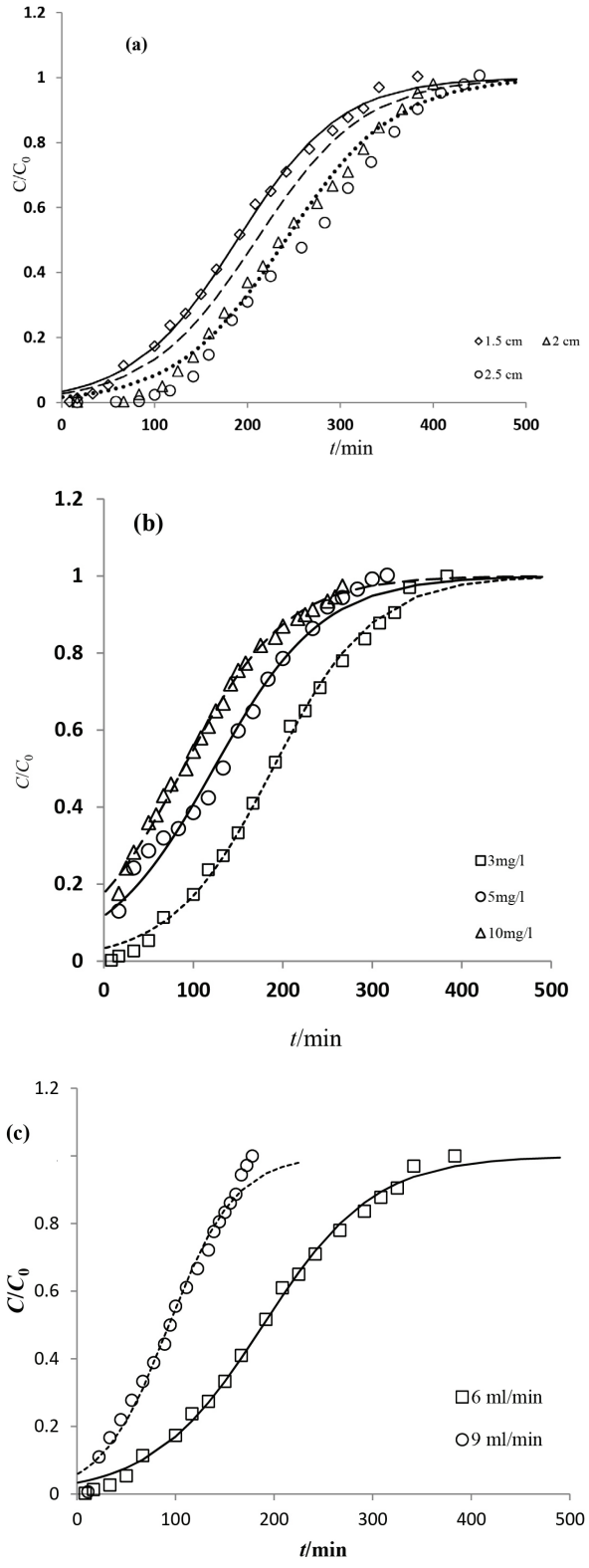

Fig. 4. Comparison of experimental, theoretical breakthrough curve and BTCs for naproxen on CD@Clay-PVP packed column using various models at different bed height (a); flow rate (b) and influent naproxen concentration (c). Experimental values are shown by data points, and model predictions are represented by lines.

3.6. Models analysis

Table 4 shows the BDST result according to plot of BDST parameters for removal of naproxen by CD@Clay-PVP at different breakthroughs and assuming that both the initial concentration, C_0 and Q, are constant during column operation. From these plots one can calculate BDST parameters, i.e., N_o and k_0 from their slopes and intercepts, and R^2 values indicate that how these adsorption systems follow the BDST equation. A good correlation for all plots ($R^2 > 0.97$) indicating the applicability of the model for predicting the service time of the adsorbents used in the column. The results are listed in Table 4.

The rate constant (k_0), calculated from the intercept of BDST plots, characterizes the rate of solute transfer from the fluid phase to the solid phase [52]. It is stated that if k_0 is large, then even a short bed will avoid breakthrough, but if k_0 decreases, a progressively longer bed is required to avoid breakthrough [30]. The BDST model parameters can be useful to scale up the process for other flow rates without further experimental runs.

On the other hand, the minimum bed height corresponding to time $t = 0$ may be predicted from the plot. The minimum bed heights were calculated and tabulated in Table 5 for various C_t/C_0.

Table 4
BDST parameters at different conditions for the adsorption of naproxen on CD@Clay-PVP using linear regression analysis

C_0 (mg/LL)	H_T (cm)	Q (mL/min)	k_0 (L mg^{-1} min^{-1})	N_0 (mg L^{-1})	U (cm min^{-1})	R^2
3	1.5	6	0.006229	2314.286	6.18	0.9867
3	2.0	6	0.005679	2246.121	6.18	0.9865
3	2.5	6	0.006080	1930.385	6.18	0.9789
3	1.5	6	0.006229	2314.286	6.18	0.9867
5	1.5	6	0.003208	2524.324	6.18	0.9776
10	1.5	6	0.001659	3623.416	6.18	0.9978
3	1.5	6	0.006229	2314.286	6.18	0.9867
3	1.5	9	0.009360	1508.18	8.08	0.9949

Table 5
Regression analysis of service time versus bed height for determination of the minimum bed height corresponding to time $t = 0$ (H_0)

C/C_0	Regression equation	N_0	k_0	H_0	R^2
0.03	$t = 68.501$ $H_T - 100.6$	1270.01	0.03455	1.469	0.9804
0.05	$t = 69.199$ $H_T - 72.391$	1282.95	0.04067	1.046	0.9850
0.08	$t = 69.857$ $H_T - 45.752$	1295.15	0.05338	0.655	0.9925
0.10	$t = 70.179$ $H_T - 32.747$	1301.12	0.06710	0.467	0.9978

A linear regression analysis was used to evaluate the Thomas model parameters and the results are presented in Table 6 at different column conditions. As listed in this table, when the bed height was increased, the value of k_{Th} decreased, and the value of q_0 increased. On the other hand, the k_{Th} value was increased from 5.6 to 9.0 mL min^{-1} mg^{-1} with increasing flow rate while the q_0 shows an opposite trend and decreased from 2.378 to 1.524 mg g^{-1} [48,53].

The comparison of the experimental and predicted breakthrough curves at different bed heights and flow rates were investigated. According to these results, lower flow rate and higher bed height was benefit to adsorption of naproxen on CD@Clay-PVP adsorbent column.

A linear plot of Eq. (7) was used to evaluate the model. The calculated parameters, k_{YN} (a rate constant), τ (t value at 50% breakthrough), and other statistical parameters for different conditions containing the inlet naproxen concentration, bed height, and flow rate are listed in Table 7.

As shown in Table 7, the k_{YN} value generally decreased with increasing inlet naproxen concentrations, whereas the τ decreased due to a rapid saturation of the column with the increasing inlet naproxen concentration. Furthermore, it was found that the K_{YN} decreased with increasing bed height, but it increases proportionally with flow rate. The τ showed an opposite trend. The correlation coefficients between the experimental and predicted values using the Yoon–Nelson model for all tested conditions were between 0.9846 and 0.9985.

A linearized form of Clark equation [Eq. (11)] was analyzed by linear regression analysis to calculate parameters A and r. The parameter values, for different conditions of inlet naproxen concentration, bed height, and flow rate are listed in Table 8. As shown in Table 8, the value of A was found to increase with increasing bed height, but it decreases proportionally with flow rate and initial concentration, whereas the r value showed an opposite trend.

As seen in Table 8, R^2 values were high (0.9646–0.997) indicating that the Clark model is good predicts for the breakthrough curve of naproxen adsorption process, meanwhile, the behavior of this system was simulated as a Freundlich adsorption.

3.7. Comparison between applied models

The predicted and experimental breakthrough curves are presented in Fig. 4. As can be seen, the experimental data are in good agreement with curve fitting from models. The fitting of models with experimental data confirms the control of external mass transfer in the initial part of breakthrough curves.

The column adsorption model applied in this study to fit the naproxen adsorption data can be essentially grouped based on their equations. It is obvious that only the characteristic parameters associated with these models varies but all the four models will predict essentially the same C_t/C_0 values for a particular data set, and are bound to give the same error function values as illustrated in Table 9. But, the prominent and unique characteristic features of the respective models enable further comparison. According to given results obtained by error analysis including R^2 values and other statistical parameters like *RMSE*, *SSE*, *SAE*, *ARE* and *ARS*, one can easily conclude that these four models are essentially the same. So, if the simulated results presented in a figure all data points overlap each other. Of course, the profitability of each model is obtaining useful parameters to evaluate the performance of the used fixed bed column.

Table 6
Thomas model parameters at different conditions for the adsorption of naproxen on CD@Clay-PVP using linear regression analysis

C_0 (mg/LL)	H_T (cm)	Q (mL/min)	k_{Th} (mL/min mg)	q_0 (mg/g)	R^2
3	1.5	6	5.60	2.378	0.9985
3	2.0	6	5.40	2.907	0.9840
3	2.5	6	5.20	3.381	0.9740
3	1.5	6	5.60	2.378	0.9985
5	1.5	6	4.08	3.992	0.9895
10	1.5	6	1.68	5.193	0.9978
3	1.5	6	5.60	2.378	0.9985
3	1.5	9	9.00	1.524	0.9953

Table 7
Yoon–Nelson parameters at different conditions for the adsorption of naproxen on CD@Clay-PVP using linear regression analysis

C_0 (mg/LL)	H_T (cm)	Q (mL/min)	k_{YN} (min^{-1})	τ (min)	R^2
3	1.5	6	0.0167	189.16	0.9985
3	2.0	6	0.0158	238.65	0.9879
3	2.5	6	0.0146	259.37	0.9896
3	1.5	6	0.0167	189.16	0.9985
5	1.5	6	0.0164	125.35	0.9846
10	1.5	6	0.0163	86.44	0.9969
3	1.5	6	0.0167	189.16	0.9985
3	1.5	9	0.0279	93.41	0.9949

Table 8
Parameters of the Clark model at various bed heights, flow rates, and initial naproxen concentrations for the adsorption of naproxen on CD@Clay-PVP using linear regression analysis

C_0 (mg/LL)	H_T (cm)	Q (mL/min)	r	A	R^2
3	1.5	6	0.0144	4.684	0.9939
3	2.0	6	0.0137	8.601	0.9874
3	2.5	6	0.0134	10.481	0.9798
3	1.5	6	0.0144	4.684	0.9939
5	1.5	6	0.0146	1.717	0.9646
10	1.5	6	0.0149	1.159	0.9970
3	1.5	6	0.0144	4.684	0.9939
3	1.5	9	0.0214	2.285	0.9931

Table 9
Error functions for prediction of breakthrough curve at various bed column conditions for all models

C_0 (mg/L)	Q (ç)	H_T (cm)	R^2	*RMSE*	*SSE*	*SAE*	*ARE*	*ARS*
3	6	1.5	0.9963	0.0219	0.0089	0.3557	0.994	3.502
3	6	2.0	0.9913	0.0328	0.0193	0.5673	1.519	4.302
3	6	2.5	0.9922	0.0344	0.0207	0.5644	3.593	10.449
3	6	1.5	0.9963	0.0219	0.0089	0.3557	0.994	3.502
5	6	1.5	0.9866	0.0351	0.0197	0.5037	0.066	0.095
10	6	1.5	0.9952	0.0179	0.00562	0.2927	0.0282	0.065
3	6	1.5	0.9963	0.0219	0.0089	0.3557	0.994	3.502
3	9	1.5	0.987	0.0359	0.0245	0.5477	0.568	2.454

4. Conclusions

In the present study, we used a synthesized clay-polymer nanocomposite functionalized with β-cyclodextrin as effective and inexpensive adsorbent to remove naproxen from aqueous solutions. From fixed-bed column experiments, it was found that the CD@Clay-PVP composite exhibited favorable adsorption of naproxen in solution. The effects of various column operating parameters, such as bed height, flow rate, and initial naproxen concentration on the adsorption capacity and breakthrough curve profiles were investigated. It was found that the adsorption capacity was increased with increasing influent concentration, but decreased with increasing the bed depth and flow rate. Thomas, BDST, Yoon–Nelson and Clark models were applied to the experimental data obtained from dynamic studies performed in the fixed bed column for the prediction of the breakthrough curves and to determine the characteristic parameters of the naproxen adsorption on CD@Clay-PVP composite under varying experimental conditions.

Prominent and unique characteristic features of the respective models like BDST, Thomas, Yoon-Nelson and Clark models were determined by adopting from regression technique. All models were found to be suitable for fitting experimental data with respect to various bed heights, flow rates, and initial naproxen concentration values. From the comparison studies it was also observed that the adsorption capacity of the present adsorbent is well compared to other similar adsorbents reported in literature.

Acknowledgments

The authors greatly acknowledge Shahid Sadoughi University of Medical Sciences for the financial support from the Grant Research Council.

References

[1] B. Petrie, R. Barden, B. Kasprzyk-Hordern, A review on emerging contaminants in wastewaters and the environment: Current knowledge, understudied areas and recommendations for future monitoring, Water Res., 72 (2015) 3–27.
[2] M. Carballa, F. Omil, J.M. Lema, M. Llompart, C. García-Jares, I. Rodríguez, M. Gómez, T. Ternes, Behavior of pharmaceuticals, cosmetics and hormones in a sewage treatment plant. Water Res., 38 (2004) 2918–2926.
[3] C. Vogelsang, M. Grung, T.G. Jantsch, K.E. Tollefsen, H. Liltved, Occurrence and removal of selected organic micropolluants at mechanical, chemical and advanced wastewater treatment plants in Norway. Water Res., 40 (2006) 3559–3570.
[4] V. Geissen, H. Mol, E. Klumpp, G. Umlauf, M. Nadal, M. Van der Ploeg, S.E.A.T.M. Van de Zee, C.J. Ritsema, Emerging pollutants in the environment: A challenge for water resource management. Int. Soil Water Conserv. Res., 3 (2015) 57–65.
[5] R. Rosal, A. Rodriguez, J.A. Perdigon-Melon, A. Petre, E. Garcia-Calvo, M.J. Gomez, A. Aguera, A.R. Fernandez-Alba, Occurrence of emerging pollutants in urban wastewater and their removal through biological treatment followed by ozonation. Water Res., 44 (2010) 578–588.
[6] T. Deblonde, C. Cossu-Leguille, P. Hartemann, Emerging pollutants in wastewater: A review of the literature. Int. J. Hyg. Environ. Health., 214 (2011) 442–448.
[7] M. Bedner, W.A. Maccrehan, Transformation of acetaminophen by chlorination produces the toxicants 1,4–benzoquinone and N-acetyl-p-benzoquinone imine. Environ. Sci. Technol., 40 (2006) 516–522.
[8] S.C. Antunes, R. Freitas, E. Figueira, F. Gonçalves, B. Nunes, Biochemical effects of acetaminophen in aquatic species: edible clams Venerupis decussata and Venerupis philippinarum. Environ. Sci. Pollut. Res. Int., 20 (2013) 6658–66.
[9] D.R. Dietrich, S.F. Webb, T. Petry, Hot spot pollutants: pharmaceuticals in the environment. Toxicol. Lett., 131 (2002) 1–3.
[10] J. Radjenovic, M. Petrovic, F. Ventura, D. Barcelo, Rejection of pharmaceuticals in nanofiltration and reverse osmosis membrane drinking water treatment. Water Res., 42 (2008) 3601–3610.
[11] W. Wang, M. Li, Q. Zeng, Adsorption of chromium (VI) by strong alkaline anion exchange fiber in a fixed-bed column: Experiments and models fitting and evaluating. Sep. Purif. Technol., 149 (2015) 16–23.
[12] R. Rostamian, M. Najafi, A.A. Rafati., Synthesis and characterization of thiol-functionalized silica nanohollow sphere as a novel adsorbent for removal of poisonous heavy metal ions from water: Kinetics, isotherms and error analysis. Chem. Eng. J., 171 (2011) 1004–1011.
[13] V.K. Gupta, D. Pathani, S. Sharma, S. Agarwal, P. Singh Remediation of noxious chromium (VI) utilizing acrylic acid grafted lignocellulosic adsorbent. J. Mol. Liq., 177(2013) 343–352.
[14] R.L. Fernández, J.A. McDonald, S.J. Khan, P. Le-Clech, Removal of pharmaceuticals and endocrine disrupting chemicals by a submerged membrane photocatalysis reactor (MPR). Sep. Purif. Technol., 127 (2014) 131–139.
[15] H.Y. Shu, M.C. Chang, J.J. Liu, Cation resin fixed-bed column for the recovery of valuable THAM reagent from the wastewater. Process Saf. Environ., 104 (2016) 571–586.
[16] M.S. Karmacharya, V.K .Gupta, I. Tyagi, S. Agarwal, V.K. Jha. Removal of As (III) and As (V) using rubber tire derived activated carbon modified with alumina composite. J. Mol. Liq., 216 (2016) 836–844.

[17] K. Rahmani,M.A. Faramarzi, A.H. Mahvi, M. Gholami, A. Esrafili, H. Forootanfar, M. Farzadkia, Elimination and detoxification of sulfathiazole and sulfamethoxazole assisted by laccase immobilized on porous silica beads, Int. Biodeterior. Biodegrad., 97 (2015) 107–114.
[18] G.H. Safari, M. Hoseini, M. Seyedsalehi, H. Kamani, J. Jaafari, A.H. Mahvi, Photocatalytic degradation of tetracycline using nanosized titanium dioxide in aqueous solution, IJEST., 12 (2014) 603–616.
[19] R. Dalvand, M. Nabizadeh, M. Reza Ganjali, S. Khoobi, A.H. Nazmara, Mahvi, Modeling of Reactive Blue 19 azo dye removal from colored textile wastewater using L-arginine-functionalized Fe_3O_4 nanoparticles: Optimization, reusability, kinetic and equilibrium studies, J Magn Magn Mater., 404 (2016) 179–189.
[20] J.L. Gong, Y.L. Zhang, Y. Jiang, G.M. Zeng, Z.H. Cui, K. Liu, C.H. Deng, Q.Y. Niu, J.H. Deng, Huan S.Y. Continuous adsorption of Pb(II) and methylene blue by engineered graphite oxide coated sand in fixed-bed column. Appl. Surf. Sc., 330 (2015) 148–157.
[21] G. Nazari, H. Abolghasemi, M. Esmaieli, E. Sadeghi Pouya., Aqueous phase adsorption of cephalexin by walnut shell-based activated carbon: A fixed-bed column study. Appl. Surf. Sci., 375 (2016) 144–153.
[22] J. Cruz-Olivares, C. Pérez -Alonso, C. Barrera-Díaz, F. Ureña-Nuñez, M. Chaparro-Mercado, B. Bilyeu., Modeling of lead (II) biosorption by residue of allspice in a fixed-bed column. Chem. Eng. J., 228 (2013) 21–27.
[23] P.N. Diagboya, E.D. Dikio, Scavenging of aqueous toxic organic and inorganic cations using novel facile magneto-carbon black-clay composite adsorbent. J. Clean. Prod., 10 (2018) 71–80.
[24] L. Rafati, M.H. Ehrampoush, A.A. Rafati, M. Mokhtari, A.H. Mahvi, Modeling of adsorption kinetic and equilibrium isotherms of naproxen onto functionalized nano-clay composite adsorbent. J. Mol. Liq., 224 (2016) 832–841
[25] L. Rafati, M.H. Ehrampoush, A.A. Rafati, M. Mokhtari, A.H. Mahvi, Removal of ibuprofen from aqueous solution by functionalized strong nano-clay composite adsorbent: kinetic and equilibrium isotherm studies. Int. J. Environ. Sci. Technol., 15 (2018) 513–524.
[26] P. Agrawal, A. Bajpai, Dynamic column adsorption studies of toxic Cr(VI) ions onto iron oxide loaded gel-atin nanoparticles. J. Dispersion. Sci .Technol., 32 (2011) 1353–1362.
[27] J. Nwabanne, P. K. Igbokwe, Adsorption performance of packed bed column for the removal of lead (ii) using oil palm fibre. Int. J. Appl. Sci. Technol., 2 (2012) 106–115.
[28] A. Shak, S. Dawood, T.K. Sen, Performance and dynamic modelling of mixed biomass-kaolin packed bed adsorption column for the removal of aqueous phase methylene blue (MB) dye, Desal. Water Treat., 81 (2017) 67–80.
[29] M.T. Yagub, T.K.S. Sen Afroze, H.M. Ang, Fixed Bed Dynamic Column Adsorption Study of Methylene Blue (MB) onto Pine Cone, Desal. Water Treat., 55 (2015) 1026–1039.
[30] M. La Farre, I. Ferrer, A. Ginebred, M. Figueras, L. Olivella, L. Tirapu, M. Vilanova, D. Barcelo, Determination of drugs in surface water and wastewater samples by liquid chromatography-mass spectrometry: methods and preliminary results including toxicity studies with Vibrio fischerim. J. Chromatogr. A., 938 (2001) 187–197
[31] R.A. Hutchins, New methods simplifies design of activated carbon system. J. Am. Chem. Eng., 80 (1973) 133–138.
[32] G.S. Bohart, E.Q. Adams, Some Aspects of the Behavior of Charcoal with Respect to Chlorinem, J. Chem. Soc., 42 (1920) 523–529.
[33] H.C. Thomas, Heterogeneous ion exchange in a flowing system. J. Am. Chem. Soc., 66 (1944) 1466–1664.
[34] C.M. Futalan, C.C. Kan, M.L. Dalida, C. Pascua, W.M. Wan, Fixed-bed column studies on the removal of copper using chitosan immobilized on bentonite. Carbohydr. Polym., 83 (2011) 697–704.
[35] N.A. Oladoja, J.E. Drewes, B. Helmreich, Assessment of fixed bed of aluminum infused diatomaceous earth as appropriate technology for groundwater defluoridation, Sep. Purif. Technol., 153 (2015) 108–117.
[36] Y.H. Yoon, J.H. Nelson, Application of gas adsorption kinetics I. A theoretical model for respirator cartridge service life, Am. Ind. Hyg. Assoc. J., 45 (1984) 509–516.
[37] Z. Aksu, F. Gönen, Biosorption of phenol by immobilized activated sludge in a continuous packed bed: prediction of breakthrough curves. Process Biochem., 39 (2004) 599–613.
[38] S.R. Pilli, V.V. Goud, K. Mohanty, Biosorption of Cr (VI) on immobilized Hydrilla verticillata in a continuous up-flow packed bed: prediction of kinetic parameters and breakthrough curves. Desal. Water Treat., 50 (2012) 115–124.
[39] R.M. Clark, Evaluating the cost and performance of field-scale granular activated carbon systems, Environ. Sci. Technol., 21 (1987) 573–580.
[40] O. Hamdaoui, Dynamic sorption of methylene blue by cedar sawdust and crushed brick in fixed bed columns, J. Hazard. Mater., 138 (2006) 293–303.
[41] N.K. Lazaridis, T.D. Karapantsios, D. Georgantas, Kinetic analysis for the removal of a reactive dye from aqueous solution onto hydrotalcite by adsorption. Water Res., 37 (2003) 3023–3033.
[42] R. Leyva-Ramos, L.A. Bernal-Jacome, I. Acosta-Rodriguez, Adsorption of cadmium (II) from aqueous solution on natural and oxidized corncob, Sep. Purif. Technol., 45 (2005) 41–49.
[43] Z. Aksu, I. Alper İşoğlu, Removal of copper (II) ions from aqueous solution by biosorption onto agricultural waste sugar beet pulp. Process Biochem., 40 (2005) 3031–3044.
[44] S. Kundu, A.K.Gupta, Arsenic adsorption onto iron oxide-coated cement (IOCC): regression analysis of equilibrium data with several isotherm models and their optimization. Chem. Eng. J., 122 (2006) 93–106.
[45] H. Lee, D.S. Kim, Preparation and physical properties of wood/polypropylene/clay nanocomposites, J. Appl. Polym. Sci., 111 (2009) 2769–2776.
[46] C. Ravindra Reddy, A. Pouyan Sardashti, L.C. Simon, Preparation and characterization of polypropylene–wheat straw–clay composites, Compos. Sci. Technol., 70 (2010) 1674–1680.
[47] K. Vijayaraghavan, J. Jegan, K. Palanivelu, M. Velan, Removal of nickel (II) ions from aqueous solution using crab shell particles in a packed bed up-flow column, J. Hazard. Mater., 113 (2004) 223–230.
[48] S.S. Baral, N. Das, T.S. Ramulu, S.K. Sahoo, S.N. Das, G.R. Chaudhury, Removal of Cr (VI) by thermally activated weed Salvinia cucullata in a fixed-bed column. J. Hazard. Mater., 161 (2009) 1427–1435.
[49] A.A. Ahmad, B.H. Hameed, Fixed-bed adsorption of reactive azo dye onto granular activated carbon prepared from waste, J. Hazard. Mater., 175 (2010) 298–303.
[50] J. Song, W. Zou, Y. Bian, F. Su, R. Han, Adsorption characteristics of methylene blue by peanut husk in batch and column modes, Desalination, 265 (2011) 119–125.
[51] E. Malkoc, Y. Nuhoglu, M. Dundar, Adsorption of chromium (VI) on pomacean olive oil industry waste: batch and column studies. J. Hazard. Mater., 138 (2006) 142–151.
[52] D.O. Cooney, Adsorption Design for Wastewater Treatment, CRC Press, Boca Raton, 1998.
[53] S. Afroze, T. Kanti Sen, H.M. Ang, Adsorption performance of continuous fixed bed column for the removal of methylene blue (MB) dye using Eucalyptus sheathiana bark biomass, Res. Chem. Intermed., 42 (2016) 2343–2364.